

# CHAPTER 2

## LITERATURE SURVEY

### 2.0 Introduction

There has been a lot of research and development activities aimed towards the commercial manufacturing of battery systems based on lithium insertion cathodes and metallic lithium anodes. This effort was primarily driven by the desire for inexpensive high energy density rechargeable batteries, which could be utilized in applications ranging in size from cellular telephones and other electronic devices to electric vehicles.

Lithium batteries that do not make use of lithium metal have been known for several years, and were originally termed as “rocking chair” batteries (RCB) by Armand, (1980). The basic concept of operation for RCB’s was partially derived from concentration cells which consist of essentially identical electrodes containing different reactant concentrations, and also from carbon/carbon cells based on cation insertion in one electrode and anion insertion in the other. Shortly after the RCB concept was revealed, the concept was demonstrated using transition metal compound anodes and cathodes. In 1990, Sony Energytech Inc (Sony Lithium Ion Battery Performance Summary, 1994) announced the commercial availability of their “lithium ion rechargeable battery” based on a carbon (non-graphitic) anode and a  $\text{LiCoO}_2$  cathode. Sony has since made several iterative improvements to the performance of their particular RCB system. Several other Japanese companies have also announced commercialization of their particular Lithium ion technology (i.e., A&T Battery, Hitachi Maxell, Mitsubishi and Sanyo) (Koksbang et al., 1996). These batteries apparently all show acceptable

performance characteristics under a variety of different design applications. In a number of cases a higher specific capacity graphitic anode has replaced the non-graphitic type used in the original Sony configuration. Furthermore, prismatic designs as well as cylindrical ones are now commercially available.

## 2.1 Lithium Manganese Dioxide

Studies on lithium cells began since 1960's, supported by NASA and the American DOD, in order to develop high power density batteries for space and military usage. At that time, alkaline metals such as Li, Na, Al and Mg were being tested as prospective anode materials from the stand point of the electrode potential and electrochemical equivalent (Gabano, 1983). Halogenides, sulphides and oxides of transition metals were examined as possible active cathode materials. High ion conductivity materials, that is those having high dielectric constant, low viscosity and at the same time stability with respect to the electrodes, were investigated for use as the electrolyte. In many systems, however, the investigation did not obtain full results with respect to stability, safety and economy.

Manganese dioxide ( $\text{MnO}_2$ ), which has been used for a long time as an active cathode material in manganese or alkaline dry-batteries, is well characterized, and known as an economical material. Lithium cells employing  $\text{MnO}_2$  as a cathodic material have been developed and commercialized, to fulfil the modern requirements but few successful results were obtained. Thus, until now the Li/ $\text{MnO}_2$  system has been thought of as unrealistic (Gabano, 1983).

Hunger and Heymach (1973) has reported that the reaction of  $\text{MnO}_2$  was a reduction reaction from  $\text{Mn}^{4+}$  to  $\text{Mn}^{3+}$ , with a utilization rate of 68% at a cut-off voltage of 0.9V, while the standard electromotive force was  $E^0=2.96\text{V}$ . Dey, (1973) reported that the utilization rate of up to 2V reached as being 90 to 100%, at 3.7-3.9V of open circuit voltage under the discharge rate of  $1\text{mAcm}^{-2}$ . At the same time, he reported swelling of the cells by gassing and the state of oxidation of  $\text{MnO}_2$  lowering during storage, both of which are undesirable characteristics. Dampier, (1974) obtained 29% of discharge utilization rate on the assumption of a 2-electron reaction per 1-mole  $\text{MnO}_2$ . Similar studies were done in Japan, on lithium cells employing  $\text{MnO}_2$ , also yielding unpromising results due to such problems of gas generation caused by water contained in  $\text{MnO}_2$  during the storage period. However it has been established that the lithium cell could be put into practical use by employing almost anhydrous  $\text{MnO}_2$  as the cathode material for non-aqueous lithium cells. In 1976, these cells were successfully commercialized. The use of this system has expanded markedly and has been adopted for production by 11 companies in the world, since 1980 (Gabano, 1983).

### 2.1.1 Properties of $\text{MnO}_2$ (MD)

$\text{MnO}_2$  has been used as the main material for dry batteries since 1860. It is the most suitable cathode material for lithium cells. There are two kinds of  $\text{MnO}_2$ , i.e. the natural ore (NMD) and synthetic  $\text{MnO}_2$ . Synthetic  $\text{MnO}_2$  can be classified as chemically prepared  $\text{MnO}_2$  (CMD) and electrolytic  $\text{MnO}_2$  (EMD) depending on their process of

production. The physical, chemical and electrical properties of these MDs are very different from one another. There are various kinds of MDs e.g. cryptomelane, nustite, psilomelane, silomelane, pyrolusite and ramsdellite. Their chemical composition is  $(K.Mn^2)(Mn^4)_8O_{16}.2H_2O$ ,  $\rho$ - (or  $\gamma$ ) $MnO_2$ ,  $MnO_2 + Ba + H_2O$ ,  $\beta$ -  $MnO_2$  and  $\gamma$ -  $MnO_2$ , respectively.  $\beta$ -  $MnO_2$  (pyrolusite) has a tetragonal structure, ramsdellite has an orthorhombic structure and  $\gamma$ -  $MnO_2$  (nustite) has a hexagonal or orthorhombic structure.

Consumption of synthetic MD, especially EMD is increasing rapidly with the requirements of high performance batteries, as the resources of high quality natural ore are decreasing. EMD consist mainly of carbonic manganese ore and MD. The crystal structure of EMD is called  $\gamma$ - $MnO_2$  and has great porosity. From an electrochemical point of view, it has high depolarizing characteristics and is mainly used as the cathodic material for high performance dry batteries (Gabano, 1983).

### 2.1.2 Reaction Mechanism

Manganese dioxide heat treated in shows  $\gamma$ -phase between room temperature and  $250^\circ C$ ,  $\gamma$  and  $\beta$ -phases between  $250^\circ C$  and  $350^\circ C$ , and  $\beta$ -phase over  $350^\circ C$ . It is important that there is no water in cathodic materials when used in non-aqueous cells, but the presence of a little water is unavoidable when  $MnO_2$  is used as active material. However, it is considered that this water is bound in the crystal structure and has no effect on the storage characteristics.

When  $\text{MnO}_2$  was heat treated at the temperatures  $100^\circ\text{C}$ ,  $250^\circ\text{C}$ ,  $350^\circ\text{C}$  and  $450^\circ\text{C}$  the open circuit and initial discharge voltages were lower if the heating temperature was high. The maximum discharge capacity is obtained at  $350^\circ\text{C}$  at a 2.0 V cut-off. When the cell was constructed using  $\text{MnO}_2$  heat treated at temperatures lower than  $250^\circ\text{C}$ , the cell case became corroded and leakage occurred. Thus, heat treatment over  $250^\circ\text{C}$  seems to be necessary when  $\text{MnO}_2$  is used as the cathodic material in non-aqueous cells.

### 2.1.3 Discharge Mechanism

Studies about the discharge mechanism of  $\text{MnO}_2$  electrodes in non-aqueous cells have been carried out using X-ray diffraction, atomic absorption spectroscopy (AAS) and ion microanalysis (IMA) methods (Gabano, 1983). A mixture of the  $\gamma$  and  $\beta$  phases of  $\text{MnO}_2$  exhibits the best discharge characteristics.  $\alpha$ - $\text{MnO}_2$  gave the poorest results .

The X-ray diffraction patterns of various stages of the discharge of  $\gamma$ - $\text{MnO}_2$  shows that the peaks at 0% utilization shift to lower angles; that is, an expansion of the crystal lattice is observed. For the discharge of  $\gamma$ - $\beta$ - $\text{MnO}_2$  the  $\gamma$  and  $\beta$  phases are still recognized at 26% utilization. However, at 52% and 78% utilization, an expansion of the crystal lattice is observed as  $\gamma$ - $\text{MnO}_2$ . For the discharge of  $\beta$ - $\text{MnO}_2$ , the peak position at 26% utilization is not different from the peak position at 0% utilization, but crystal structure weakens. At 52% and 78% utilization, a shift to a low angle, namely, an expansion of the

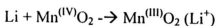
crystal lattice, is observed. For the discharge of  $\alpha$ - $\text{MnO}_2$ , the crystal structure at 26% utilization becomes weaker than at 0% utilization.

The cell with configuration  $\text{Li}/\text{MnO}_2$  with a liquid electrolyte was expected to proceed according to the following reaction



However, such cells did not obey the above equation as  $\text{Mn}_2\text{O}_3$  and  $\text{Li}_2\text{O}$  were not found in the X-ray diffraction patterns of the electrodes and the open-circuit potential is different from the reversible potential  $E^0$  of 2.69V. The X-ray diffraction patterns show a shift of the peak to a lower angle, demonstrating an expansion of the crystal lattice, as the discharge proceeds.

AAS also shows that the Li content corresponding to the discharge amount is found in the cathode mixture. Thus, the reaction of  $\text{Li}/\text{MnO}_2$  in a non-aqueous electrolyte is assumed to be as follows



$\text{MnO}_2(\text{Li}^+)$  signifies that  $\text{Li}^+$  ion was introduced into the  $\text{MnO}_2$  crystal lattice. The  $\text{Li}^+$  ion seems to behave like proton in aqueous solution.

### 2.1.4 Manganese Dioxide Reactions

The diffusion of  $\text{Li}^+$  ion into the  $\text{MnO}_2$  crystal lattice, the relationship between cell characteristics and  $\text{MnO}_2$  content, water content and surface area, with the crystal structure and products analysed using XRD and IMA will be discussed in this section. The results for the different types of  $\text{MnO}_2$ , EMD, NMD, CMD and nearly anhydrous  $\text{MnO}_2$  (MEMD) treated by microwave irradiation, are also described.

#### 2.1.4.1 $\text{MnO}_2$ and Water Content

The  $\text{MnO}_2$  content in EMD, NMD, CMD and MEMD are 91.8%, 80.7%, 93.6% and 92.4% while the water content is 5.55%, 3.15%, 2.97% and 3.07% respectively.

#### 2.1.4.2 Crystal Structure of $\text{MnO}_2$

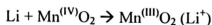
X-ray diffraction patterns showed that  $\text{MnO}_2$  was in the  $\gamma$ -phase from room temperature to  $250^\circ\text{C}$ , undergoing  $\gamma$  to  $\beta$ -phase transition at  $250^\circ\text{C}$  to  $350^\circ\text{C}$ , and in the  $\beta$ -phase at over  $350^\circ\text{C}$ . X-ray diffraction patterns of CMD, NMD and MEMD before and after heat treatment ( $400^\circ\text{C}$ ) showed that all the  $\text{MnO}_2$  were in the  $\gamma$ -phase originally. NMD has sharp peaks and is expected to have a better crystalline structure. MEMD was still preserved in  $\gamma$ -phase even after the heat treatment. All other types of  $\text{MnO}_2$  that were heat treated at  $400^\circ\text{C}$  were in the  $\beta$ -phase.

### 2.1.4.3 Discharge Characteristics of Test Cell

The discharge curves of cells using different types of  $\text{MnO}_2$  have been obtained for a load of  $12\text{k}\Omega$ . Stable discharge curves were obtained for cells employing EMD, MEMD and CMD as cathode materials. The discharge time of cell with NMD as the cathode material is less than for those using other types of  $\text{MnO}_2$ . Discharge performance at  $5.6\text{k}\Omega$  had the same relative results.

In the cells using EMD, CMD and MEMD, which have over 90%  $\text{MnO}_2$  content, almost 100% utilization was obtained and 90% utilization was obtained even in the cell using NMD. These results correspond well with theoretical capacity estimated, based on a one electron reaction mechanism and the cell reaction mechanism was thus confirmed. In  $\text{Li}/\text{MnO}_2$  cells, discharge characteristics correspond well with  $\text{MnO}_2$  content, and the suitability of a  $\text{MnO}_2$  can be judged roughly from the  $\text{MnO}_2$  content.

X-ray diffraction on all of these  $\text{MnO}_2$  except natural  $\text{MnO}_2$  indicated a broadening and shift of their peaks as discharge proceeded. Natural  $\text{MnO}_2$  showed little peak shifting, but intensities of the peaks became weaker as discharge proceeded. It is believed that this is caused by reduction of tetra-valent Mn to tri-valent Mn, as shown by the equation





This could be explained by  $\text{Li}^+$  ions being introduced into the crystal lattice of  $\text{MnO}_2$ , which can be confirmed by the results of X-ray diffraction where  $\text{Li}_2\text{O}$  could not be detected. The results of IMA lend further support for the discharge reaction mechanism of  $\text{MnO}_2$ . This reaction model is applicable for  $\gamma$ ,  $\gamma$ - $\beta$  and  $\beta$ -phase  $\text{MnO}_2$  produced by different processes.

## 2.2 $\text{LiMn}_2\text{O}_4$

Much of the available work has concentrated on the spinel phase  $\text{Li}_x\text{Mn}_2\text{O}_4$ . Although this review is, primarily concerned with the high voltage materials (i.e. those best suited for the rocking chair batteries), some materials operating at the 3V plateau will also be included. Significant efforts are also underway to extend the capacity of the 4V plateau to the 3V plateau without significantly compromising the specific capacity. The structure of the  $\text{LiMn}_2\text{O}_4$  compound is described in (Wells, 1984), and is reviewed together with the structures of related manganese oxides, as well as other spinel compounds, in (Thackeray, 1995). Structural work on the delithiated spinels is also found in (Mosbah, 1983; Hunter, 1981). The  $\text{LiMn}_2\text{O}_4$  spinel is by far the most extensively investigated manganese oxide, both for the 3V plateau, the 4V plateau, or for both plateaus. In a few cases up to 4 Li per  $\text{Mn}_2\text{O}_4$  unit have been cycled. In this particular case the cycling has been extended to include the lowest voltage plateau around 1V versus Li. The major emphasis in this review is concentrated on the parent  $\text{LiMn}_2\text{O}_4$  spinel compound and its derivatives (Koksang et al., 1996).

### 2.2.1 $\text{LiMn}_2\text{O}_4$ , 4V plateau

The cycling of the 1 Li per  $\text{Mn}_2\text{O}_4$  unit corresponds to a theoretical material utilization capacity of 148 mAh/g. This figure is somewhat lower than the corresponding value for the cobalt and nickel  $\text{LiMO}_2$  phases (Koksang et al., 1996). In most experimental cells, it is found that the reversible specific capacity of the 4V range for the  $\text{LiMn}_2\text{O}_4$  is about 120mAh/g, or about 81% of the theoretical capacity. The theoretical capacity may be reached at very low cycling rates, although extended cycling at these rates is normally accompanied by a concurrent capacity fade.

The  $\text{LiMn}_2\text{O}_4$  compound is traditionally made by annealing of the corresponding carbonates in the approximate temperature range 700-900°C. Other synthesis routes, primarily encompassing different low temperature methods based on sol-gel chemistry, have been investigated. Sol-gel synthesis of manganese oxides is discussed in details in (Tsumura et al., 1993; Bach et al., 1990; Pereira, 1995; Pereira et al., 1995a). As in the case of the  $\text{LiMO}_2$  compound, only minor performance improvements in terms of specific capacity or cycling, (or none at all), are observed. Li et al., (1994; 1995), demonstrated lithium insertion in  $\text{LiMn}_2\text{O}_4$  from an aqueous electrolyte.

For application purposes it has been necessary to unequivocally demonstrate long term cycling of the  $\text{LiMn}_2\text{O}_4$  material without significant capacity fade. To that end, Tarascon and Guyomard (1993) had demonstrated that it is possible to retain a capacity around 75mAh/g for  $\text{LiMn}_2\text{O}_4$  after more than 1000 deep discharge cycles. Furthermore

(Shokoohi et al., 1995) have shown a full RCB that incorporates the spinel cathode coupled to a petroleum coke anode with over 1300 deep discharge cycles and only a 36% decline in the battery discharge capacity.

A study using a solid inorganic phosphate electrolyte, which is stable above 5V versus Li has been reported by Bates and co-workers (1995), indicated that structural changes which take place at very high potentials, are in some way beneficial to the capacity at the 4V plateau. It was previously shown (Shokoohi et al., 1995a; Tarascon and Guyomard (1994); Coowar et al., 1994) that two reversible redox reactions take place at high anodic potentials (4.55 and 4.95V versus Li). The additional capacity only corresponds to  $x=0.06$  for both plateaus.

### **2.2.2 $\text{LiMn}_2\text{O}_4$ , 3V plateau**

Since approximately 1 Li per  $\text{Mn}_2\text{O}_4$  unit can be inserted over the approximate 3V voltage plateau, the theoretical specific capacity of this plateau (Gummow et al., 1994; de Picciotto et al., 1984; Pistoia et al., 1992; Ohzuku et al. 1992), is roughly identical to the capacity of the 4V plateau, i.e. around 150mAh/g. However, the delivered capacity is often significantly lower than that of the 4V plateau, and the capacity fade with cycle number is usually greater. It has been reported (Barker et al. 1994; 1995) that the electrode impedance increases abruptly (almost by a factor of ten) at the transition between the 4V and the 3V plateau, which then causes lower material utilization and poor cycling properties. It was concluded that the concurrent cubic to tetragonal phase change

which accompanies lithium insertion over this voltage range, confers the inferior electrochemical performance on this material. Thackeray and co-workers (1992) also reported the poor cycling of the  $\text{Li/Li}_x\text{-Mn}_2\text{O}_4$  cells on the 3V plateau and attributed this to an asymmetric lattice expansion/contraction of the  $\text{Li}_x\text{Mn}_2\text{O}_4$  electrode during cycling. They contended that the lattice distortion resulted from a Jahn-Teller distortion that occurs around  $x=1.08$ , and transforms the cubic symmetry of the spinel phase to a tetragonal symmetry.

Methods to stabilize this Jahn-Teller distortion have been reported. For example, by varying the synthesis conditions Tarascon et al., (1991) and Barboux et al., (1992), showed that it was possible to control the amount of lithium which can be reversibly inserted/extracted within each voltage plateau. However, overall, the total amount of lithium available in both plateaus remains approximately constant. Improved performance at the 3V plateau was achieved by modification of the synthesis procedure (Huang and Bruce, 1994). The materials were prepared from  $\text{Li}_2\text{CO}_3$  and  $\text{Mn}(\text{CH}_3\text{COO})_2 \cdot 4\text{H}_2\text{O}$ , to which a small amount of carbon black powder was added. The theoretical specific capacity was achieved, and the capacity decay was smaller than that of conventionally prepared  $\text{LiMn}_2\text{O}_4$ .

Although acceptable cycling performance of cells covering both the 3V and 4V plateaus together is considered to be difficult, at least one report has appeared which indicated that this is certainly a possibility (Ouyang et al., 1995) (at least over a restricted number of discharge/charge cycles). The  $\text{LiMn}_2\text{O}_4$  material described in (Ouyang et al.,

1995) was prepared by a proprietary method and the electrochemical performance compared directly to commercially available  $\text{LiMn}_2\text{O}_4$ . The paper stresses the importance of controlling the processing conditionings for obtaining a material with both high specific capacity and improved reversibility of the lithium insertion reaction.

In one report the lithium capacity at the 3V plateau has been used as a subsidiary lithium source (Tarascon and Guyomard, 1993), in order to retain a larger fraction of the capacity at the 4V plateau, which would otherwise be consumed due to the capacity loss often observed during the initial cycling of the carbon anode (Matsumara et al., 1995). This was achieved by chemically increasing the lithium content in  $\text{Li}_{1+x}\text{Mn}_2\text{O}_4$  by the use of  $\text{LiI}$  similarly to the methods originally described by Murphy, 1980.

Finally, scale-up of cells to the AA battery size has been demonstrated (Thackeray, 1989). In this study the 3V plateau of  $\text{Li/LiMn}_2\text{O}_4$  cells was cycled more than 100 times but at low material utilisation.

### 2.3 $\text{LiCoO}_2$

The lithium cobalt oxide,  $\text{LiCoO}_2$ , was among the lithium insertion compounds first described by Mizushima and company (1980), and is currently the most extensively used cathode material for rocking chair batteries. Removal of lithium corresponding to  $x=1$  in  $\text{Li}_x\text{CoO}_2$ , is equivalent to a theoretical capacity of about 274 mAh/g. However, due to structural restrictions (Delmas, 1989), lower amounts of lithium may be removed

and inserted reversibly. The general consensus between independent researchers appears to suggest that a maximum of around 150mAh/g may be reversibly cycled over many charge-discharge cycles without appreciable specific capacity loss. In most instances groups testing under rates of insertion/extraction consistent with cell usage, report reversible specific capacities in the range 120-140mAh/g. Very high cycle numbers are obtained with commercially available batteries from Sony and others, with minimal capacity losses (Koksang et al., 1996).

Several synthesis routes have been attempted to improve the performance, including the conventional sintering of a carbonate mixture, nitrate mixture, LiOH and either a carbonate, an oxide or a nitrate of cobalt. The general trend suggests that the high temperature synthesis methods have little or no influence on the electrochemical performance of the  $\text{LiCoO}_2$  material since essentially identical results are obtained. The differences observed can probably be ascribed to electrolyte properties, choice of current collectors, or electrode preparation. Most reports on materials prepared at low temperature show only a restricted number of charge/discharge cycles. For example, an unusually high specific capacity or the low temperature material was demonstrated but unfortunately only a few cycles are reported and the long term cycle life is unknown (Koksang et al., 1996).

The structure of  $\text{LiCoO}_2$  and the structure variations during Lithium insertion and Lithium extraction, have been studied in detail. The structural differences between  $\text{LiCoO}_2$  prepared by conventional high temperature synthesis and the so called low

temperature lithium cobalt oxide (LT-  $\text{LiCoO}_2$ ) prepared at about  $400^\circ\text{C}$ , are discussed in (Gummow and Thackeray, 1993). In addition to the insertion of lithium into the  $\text{Li}_x\text{CoO}_2$  lattice, the corresponding sodium reactions were also studied (Koksang et al., 1996).

The influence on the insertion properties by the formation of interfacial layers on the  $\text{LiCoO}_2$  has been described. The formation of this cathode electrolyte interface layer, apparently formed by reaction between the electrolyte (1M  $\text{LiBF}_4/\text{PC}$ ) and the cathode components was indicated by ac impedance measurements. It is formed in an analogous fashion to the solid electrolyte interface model (SEI), originally postulated by Peled and co-workers (Peled and Gabano, 1983) to characterize the interfacial properties between metallic lithium and non-aqueous electrolytes. The cathode interfacial layer model was expected to moderate the electrochemical properties of the  $\text{LiCoO}_2$  composite electrode. The film formation was further substantiated by electron micrographs of a  $\text{LiCoO}_2$  composite cathode surface in contact with the electrolyte surface (Thomas et al., 1985).

The use of  $\text{LiCoO}_2$  as a cathode material in large test/prototype cells, has been demonstrated by several organizations (Smith et al, 1992; Beard et al., 1992; Broadhead et al. 1995; Brandt, 1995). Cylindrical 30Ah batteries constructed from plates using metallic Li anodes were cycled 40-50 times without appreciable loss of discharge capacity. Cylindrical 1.5-2 Ah and 8 Ah cells, having a flat plate construction inside (Beard et al., 1992), were assembled and tested, together with two types of spirally wound cells of 0.3-0.5Ah, and 4-6Ah capacities, respectively. In addition, prismatic 3Ah rocking chair (carbon anode) cells were also tested (Smith et al., 1992). Cylindrical "C"

size cells based on both  $\text{LiCoO}_2$  and  $\text{LiNiO}_2$  cathode materials and with a lithium anode (Broussely et al., 1993) showed high capacity and a cycle life exceeding 100 cycles.

### 2.3.1 Electrochemical Behavior

The electrochemical behavior of  $\text{LiCoO}_2$  have been studied by galvanostatic intermittent titration technique (GITT), impedance spectroscopic (IS) analysis and charge/discharge capacity measurement (Yan et al., 1998). The  $\text{Li}_{1-x}\text{CoO}_2/\text{Li}$  cell has a wide potential plateau near  $3.9 V_{\text{Li/Li}^+}$  versus  $x$ . The plateau is due to the coexistence of two pseudophase, namely, a diluted phase and a concentrated phase. Compared with conventional case, the microwave-synthesized  $\text{LiCoO}_2$  has a higher open circuit voltage  $3.87 V_{\text{Li/Li}^+}$  and flatter potential plateau.

From impedance spectra in Nyquist form, it can be observed that in the high-frequency range of 100Hz to 100kHz there is an arc which is due to reaction at the electrolyte/oxide electrode interface. In the intermediate frequency range of 5-100Hz, a clear linear part is observed that is inclined to the real axis at approximately  $45^\circ$ . It is attributed to a Warburg impedance which is associated with a semi-infinite diffusion of  $\text{Li}^+$  in the electrode. When the frequency is lower than 5 Hz, a transition from a  $45^\circ$  to an approximately  $90^\circ$  slope in the complex-plane a.c. impedance plot occurs, which is the evidence of the transition from semi-infinite to finite diffusion lengths (Li et al., 1996).



The microwave-synthesized  $\text{LiCoO}_2$  has high reversible capacity and good cyclability due to its microstructure (0.5~1.0 $\mu\text{m}$  grain size) and electrochemical characteristics (Yan et al., 1998). The initial discharge capacity is as high as 140mAh/g. The capacity loss over the first 40 cycles is less than 7% of initial discharge capacity, which is a rather good result for a  $\text{Li}/\text{LiCoO}_2$  cell.

Upon comparison of the discharge capacity for microwave synthesized  $\text{LiCoO}_2$  and for conventional solid reaction  $\text{LiCoO}_2$  at different charge/discharge current density. The microwave-synthesized  $\text{LiCoO}_2$  shows a larger capacity and a lower capacity loss at high current density. For  $\text{LiCoO}_2$  synthesized by the conventional method, when the current density increases to 2.0  $\text{mAcm}^{-2}$ , the discharge capacity is less than 50% of the initial capacity. For the microwave-synthesized  $\text{LiCoO}_2$  at the same current density, the capacity is 75% of the initial capacity. Even when the current density is 2.8  $\text{mAcm}^{-2}$ , the discharge capacity is still higher than 60%, which indicates that the microwave-synthesized  $\text{LiCoO}_2$  with fine power has the capability to withstand large current density charge and discharge.

From the report of Barker et al. (1996) a significant coulombic inefficiency was present in the first charge-discharge cycle. The second cycle data, however were close to 100% coulombic efficiency and demonstrated that around  $x=0.64$  in  $\text{Li}_x\text{CoO}_2$ , lithium could be inserted reversibly. The group also found two additional reversible differential capacity features at cell potentials of approximately 4.08V and 4.30V versus Li on charge. The kinetic investigation revealed the average diffusion coefficient for the

composite  $\text{Li}_x\text{CoO}_2$  cathode to be in the range  $10^{-9}\text{cm}^2\text{s}^{-1}$  indicating the relatively facile reaction kinetics for the lithium insertion reaction. The dc impedance data collected by the current interrupt method were broadly consistent with the ac impedance spectra and showed the presence of two distinct impedance regions dependent on the cell state-of-charge. One region exist below approximately  $x=0.6$  where the system generates relatively similar characteristics. The second region occur above about  $x=0.7$  where significantly higher impedance properties are found. The group suspect morphological changes at the Lithium/electrolyte interface to be responsible for these impedance variations.

In another study (Takada et.al., 1995), a  $\text{Li}_x\text{CoO}_2$  was examined using lithium ion conductive glass,  $\text{Li}_3\text{PO}_4\text{-Li}_2\text{S-SiS}_2$ , as the electrolyte and Li metal as the negative electrode. Complex impedance analysis showed that the electrochemical reaction rate at  $\text{Li}_x\text{CoO}_2$  electrode was mainly controlled by diffusion for  $x>0.95$  and by charge transfer for  $x<0.95$ . Coulometric titration showed that these electrode materials had specific capacities of 80-90 mAh/g, coulombic efficiencies of 100%, and equivalent voltages of around 4V versus Li, so they are promising candidates for positive electrode materials for all solid state lithium batteries.

## 2.4 $\text{LiNiO}_2$

$\text{LiNiO}_2$  exist in two structural modifications, of which only one is electrochemically active (Ohzuku, et al., 1991). The theoretical capacity of  $\text{LiNiO}_2$ ,

assuming 1 Li per  $\text{NiO}_2$  unit may be extracted, is close to that of the  $\text{LiCoO}_2$  compound, i.e.  $\approx 275 \text{mAh/g}$ . Again, in a similar fashion to the cobalt system, a significantly lower capacity is obtained in actual test cells. However, the overall reversible specific capacities reported for  $\text{LiNiO}_2$  are typically 10-30mAh/g higher than those for  $\text{LiCoO}_2$  (Koksang et al., 1996). Fewer cycles have been reported, but good charge retention is generally observed after >100 cycles. Very small particle size was claimed to be advantageous in one report, but unfortunately no electrochemical data were presented. The cycle life size is strongly dependent on the depth of discharge (Yamada et.al., 1995) i.e. high cycle numbers were achieved when the capacity was restricted to about 100 to 120mAh/g, while only a few cycles were possible at higher capacities.

In addition, the  $\text{LiNiO}_2$  compound appears to be more difficult to synthesize than the corresponding cobalt oxide, in a modification which is able to reversibly insert lithium to any significant extent. Contrary to  $\text{LiCoO}_2$ , which can be prepared by sintering a mixture of almost any Li, Co and O source under proper temperature conditions, the  $\text{LiNiO}_2$  compound needs to be prepared under strongly oxidizing conditions. Typical examples include e.g. hydroxide mixtures annealed in an  $\text{O}_2$  atmosphere, hydroxide and nitrate or by the use of  $\text{Na}_2\text{O}_2$  and an Ni source, followed by ion exchange with  $\text{LiNO}_3$  at elevated temperatures.

The structure of  $\text{LiNiO}_2$  is described in (Wells, 1984; Dahn et al. 1990; Li et al. 1994a; Hirano et al., 1995), and is discussed in (Dahn et al., 1990). The latter paper also discussed lithium insertion in the approximate range  $1 < x < 2$  in  $\text{Li}_x\text{NiO}_2$ , which takes place

at about 1.8V versus Li. This is in contrast to lithium insertion in  $\text{LiCoO}_2$  where no plateau around this voltage is found. At about 1.1V versus Li, a large plateau is observed in the  $\text{Li/LiNiO}_2$  system, presumably corresponding to the disproportionation of  $\text{LiCoO}_2$  to  $\text{Li}_2\text{O}$  and Co metal (Dahn et al., 1990).

Performance results, comparable to those of liquid electrolyte systems, were obtained with  $\text{Li/LiNiO}_2$ ,  $\text{Li/LiMn}_2\text{O}_4$ ,  $\text{C/LiNiO}_2$  and  $\text{C/LiCoO}_2$  cells (Koksang et al., 1996), using a PAN based hybrid polymer electrolyte (i.e. polymer-liquid-salt combination, (Koksang et al., 1996)) at room temperature. However, a rapid decay of the capacity with cycling, was observed in the early experiments with the carbon anode based systems. Cycle testing (Broussely et al., 1995) of a  $\text{C/LiNiO}_2$  cell, slightly smaller than a "C" size, showed good initial capacity (approximately 1Ah), and about 40% of this capacity was retained after 1200 cycles at relatively high rates.

Figure 2.1 shows the crystalline structure of  $\text{LiNiO}_2$  (Korovin, 1998). In the studies of Lee, Sun and Nahm,  $\text{LiNiO}_2$  powders were synthesized by a sol-gel method using adipic acid as a chelating agent (Lee et al., 1999). Highly crystallized  $\text{LiNiO}_2$  was synthesized in oxygen at a calcination temperature of  $750^\circ\text{C}$  for 14 hours when molar ratio of adipic acid to total metal ions was 1.0. The intensity ratio of (003)/(104) peaks of XRD spectrum for the synthesized material was 1.67. The  $\text{LiNiO}_2$  powders were monodispersed particulate with the average size of approximately 1-2 $\mu\text{m}$ . The electrochemical test of a half cell fabricated using the  $\text{LiNiO}_2$  powders revealed that

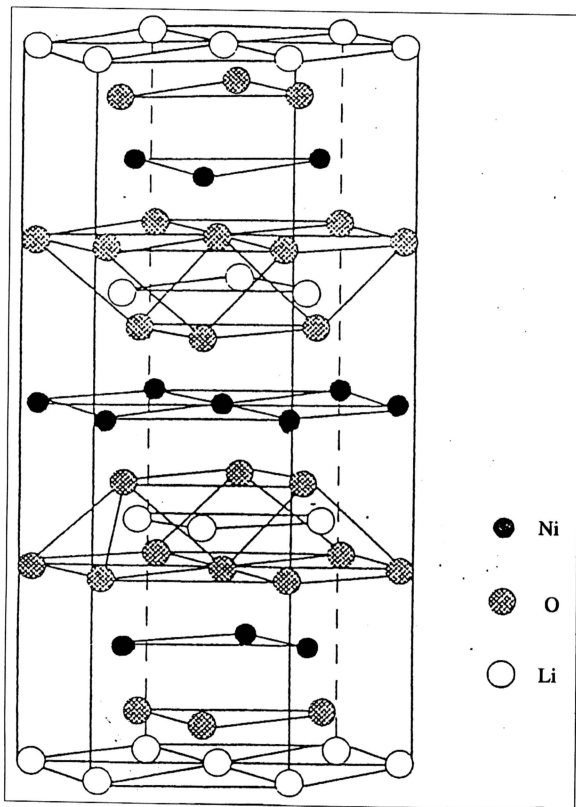


Figure 2.1 : Structure of  $\text{LiNiO}_2$ .

the cell had a high initial discharge capacity of 158 mAh/g, but it showed very fast capacity fading just after several tens of charge/discharge cycles.